

# SYNTHESIS OF $\text{Ag}@\text{Cu}_3(\text{PO}_4)_2$ -g- $\text{C}_3\text{N}_4$ FOR ELECTROCHEMICAL BIOSENSING OF BOVINE SERUM ALBUMIN

Running Title: Analyzing the biosensing activity of the fabricated  $\text{Ag}@\text{Cu}_3(\text{PO}_4)_2$ -g- $\text{C}_3\text{N}_4$  compound using bovine serum albumin assay

**M.Pranaw<sup>1</sup>, Dr. Abirami Arthanari<sup>2</sup>**

<sup>1</sup>Undergraduate, Saveetha Dental College and Hospital,  
Saveetha Institute of medical and Technical Sciences,  
Saveetha University, Chennai- 600077

<sup>2</sup>Senior Lecturer, Department of Forensic Odontology

Saveetha Dental College and Hospitals

Saveetha Institute of Medical and Technical Sciences, Chennai - 600077

Email : abiramia.sdc@saveetha.com

## Corresponding Author

**Dr. Abirami Arthanari**

Senior Lecturer, Department of Forensic Odontology

Saveetha Dental College and Hospitals

Saveetha Institute of Medical and Technical Sciences

Chennai - 600077

Email : abiramia.sdc@saveetha.com

## Abstract

**INTRODUCTION:** Electrochemical biosensing is essential for identifying and measuring biomolecules. Proteins, such as bovine serum albumin (BSA), are particularly interesting among these biomolecules due to their importance in a variety of biological processes like their potential as biomarkers for different diseases, etc.

The superior conductivity and catalytic qualities of the Ag NPs make them the perfect choice for increasing the electrochemical response by providing a conductive substrate for electron transfer. Due to their porous structure and distinctive electrical properties, the  $\text{Cu}_3(\text{PO}_4)_2$  have garnered a lot of attention and aid in the immobilization and identification of BSA molecules. The  $\text{C}_3\text{N}_4$  matrix, also known as carbon nitride, acts as a protective layer and improves the overall stability and selectivity of the biosensing platform thanks to its exceptional stability and biocompatibility. It can be used in a variety of applications, including fluorescent probes, electrochemical sensors, FETs, etc.

**AIM:** The aim of this study is to develop and characterize a novel  $\text{Ag}@\text{Cu}_3(\text{PO}_4)_2$ -g- $\text{C}_3\text{N}_4$  nanocomposite for electrochemical biosensing of bovine serum albumin (BSA).

**MATERIALS AND METHODS:** Synthesis of  $\text{Ag}@\text{Cu}_3(\text{PO}_4)_2$ -g- $\text{C}_3\text{N}_4$  Nanocomposite: The  $\text{Ag}@\text{Cu}_3(\text{PO}_4)_2$ -g- $\text{C}_3\text{N}_4$  nanocomposite is synthesized through a suitable method, such as a one-pot hydrothermal or co-precipitation process. The Ag nanoparticles are incorporated into the  $\text{Cu}_3(\text{PO}_4)_2$  matrix, which is further combined with  $\text{C}_3\text{N}_4$  to form the final nanocomposite.

**RESULTS:** XRD pattern typically exhibits characteristic peaks that correspond to the arrangement of atoms within the crystal lattice. EDS analysis shows that  $\text{Ag}@\text{Cu}_3(\text{PO}_4)_2$ -g- $\text{C}_3\text{N}_4$  consists a composition ( 37.62 % - carbon, 23.03% - nitrogen, 31.94% - oxygen, 1.93% - phosphorous and 5.48% - copper) of various components. The Fluorescence intensity shows the degree of quantification of Bovine serum albumin by the electrochemical biosensor. At a BSA concentration of (1.0, 0.8, 0.6, 0.4 and 0.2) the corresponding fluorescence intensity values are (3500 nm, 2900 nm, 2250 nm, 1750 nm and 800 nm).

**CONCLUSION:** The composite material demonstrates positive results even at low concentrations of BSA, indicating its effectiveness for detecting and quantifying BSA in various samples. Nevertheless, the research on  $\text{Ag}@\text{Cu}_3(\text{PO}_4)_2$ -g- $\text{C}_3\text{N}_4$  biosensor for BSA

detection provides a foundation for potential forensic applications in various areas of analysis and investigation.

**KEYWORDS:** Biomolecular detection,  $\text{Ag}@\text{Cu}_3(\text{PO}_4)_2$ -g- $\text{C}_3\text{N}_4$ , Composite material, Electrochemical biosensing, Bovine serum albumin, Surface morphology, Sensor development.

## INTRODUCTION

When analytes respond, electrochemical sensors create an electrical signal that is proportional to the concentration of the analyte. A sensing electrode (working electrode) and a reference electrode are typically found in an electrochemical sensor, which is divided by an electrolyte. The reference electrode is connected to a high-input-impedance potentiostat and a counterelectrode is utilized to complete the circuit for current flow in the majority of applications(1). One of the key advantages of electrochemical biosensors relies on their relative simplicity. Inexpensive electrodes can be easily integrated with simple electronics to perform rapid measurements in miniaturised easy-to-use portable systems. The ability to determine the concentration of an analyte within a complex sample at the point-of-care and in near real time is extremely attractive for medical diagnosis, monitoring of existing conditions and environmental monitoring(1,2).

A globular protein called albumin is essential for maintaining both the dietary balance and plasma pressure. As different substances bind to albumin in the blood, they are transported. Additionally, the level of serum albumin in blood plasma or other biological fluids is intimately related to human health. Bovine serum albumin (BSA), which shares a high degree of structural similarity with human serum albumin (HSA), has received extensive research as a model protein in a variety of domains. It is also referred to as a carrier protein and an allergen. Determining bovine albumin is therefore crucial in a variety of fields, including medicine, pharmaceuticals, clinical testing, and food. Therefore, it is crucial to create novel, effective, quick, and simple techniques for the selective detection of BSA(3).

Metal nanoparticles have been used in wide applications in electrochemical sensors. Among the metal nanoparticles, silver nanoparticles (AgNPs) are one of the most well-developed materials and have been used to modify the surface of working electrodes because they are inexpensive in relative comparison with those other materials, possess good chemical and physical properties, providing excellent electron transfer rates and greatly decrease the overpotential of oxidizing or reducing agents produced from enzymatic products(4). AgNPs show excellent electrocatalytic activity for  $H_2O_2$  and size distribution of AgNPs played an important role in their electrocatalytic activity(5). Silver nanoparticles (Ag NPs) have gained much research interest in biomedical applications due to excellent surface-enhanced Raman scattering (SERS), biocompatibility, high conductivity, amplified electrochemical signals, and catalytic activity. An optical fiber sensor based on both localized surface plasmon resonance (LSPR) and lossy-mode resonance (LMR) was demonstrated using Ag NPs. The devices showed high sensitivity (0.943 nm per RH %), a large dynamic range (42.4 nm for RH changes between 25% and 70%), and a fast response time (476 ms and 447 ms for rise and fall, respectively)(6).

To improve the immobilization of recognition components (such as antibodies or aptamers) for BSA detection,  $Cu_3(PO_4)_2$  is used

as a supporting substance or as part of the electrode surface modification.  $Cu_3(PO_4)_2$  has a porous structure that can offer a large surface area, enhancing BSA or recognition element binding. Additionally, the electrochemical detecting procedure may benefit from its electrical features' signal amplification or effective electron transfer(7).  $C_3N_4$  can be incorporated into electrochemical biosensors as a modified electrode material. Its excellent stability and conductive properties can improve the efficiency of electron transfer reactions involved in biosensing. This is especially useful in electrochemical detection of various biomolecules, including proteins like BSA(8).

## MATERIALS AND METHODS

**STEP1:** g- $C_3N_4$  was synthesised by a straightforward method known as direct thermal polymerization. In this process, a specific precursor material is placed inside either a ceramic crucible or a quartz boat. Subsequently, the setup is subjected to high temperatures, typically ranging around 500 °C. To ensure the success of the reaction, this heating step is carried out under an inert atmosphere (such as nitrogen or argon) or in a vacuum furnace. As a result of this controlled heating, the precursor material undergoes polymerization and condensation, leading to the formation of g- $C_3N_4$ .

**STEP2:** In an appropriate reaction vessel, combine the silver precursor (for example, silver nitrate,  $AgNO_3$ ),  $NABH_4$  as the reducing agent, and a stabilizing agent (such as a surfactant or polymer) to prevent the nanoparticles from clustering together. Thoroughly blend these constituents in the reaction vessel to achieve a consistent and even distribution.

**STEP3:** Prepare a copper precursor solution by dissolving a copper salt, like copper nitrate, in water or a suitable solvent. Simultaneously, prepare a phosphate solution by dissolving a phosphate salt, such as sodium phosphate, in water or a compatible solvent. Combine the copper precursor solution and the phosphate solution in a sealed reaction vessel. Then, raise the temperature of the reaction vessel to a specific degree (180 °C) and maintain it at this level for 16 hours to facilitate the reaction and the subsequent formation of nickel phosphate. Once the hydrothermal reaction is complete, cool down the reaction vessel and collect the resulting copper phosphate precipitate.

**STEP4:** To eliminate any impurities, cleanse the precipitate using an ethanol solvent, and then employ filtration methods to dry it. Finally, subject the dried copper phosphate to a temperature of 150 °C for 12 hours to complete the process.

**STEP5:** Add Ag nanoparticles to the materials using ultrasonication for 3 h and then filtration, dry for 3 hrs at 90 °C.

RESULTS

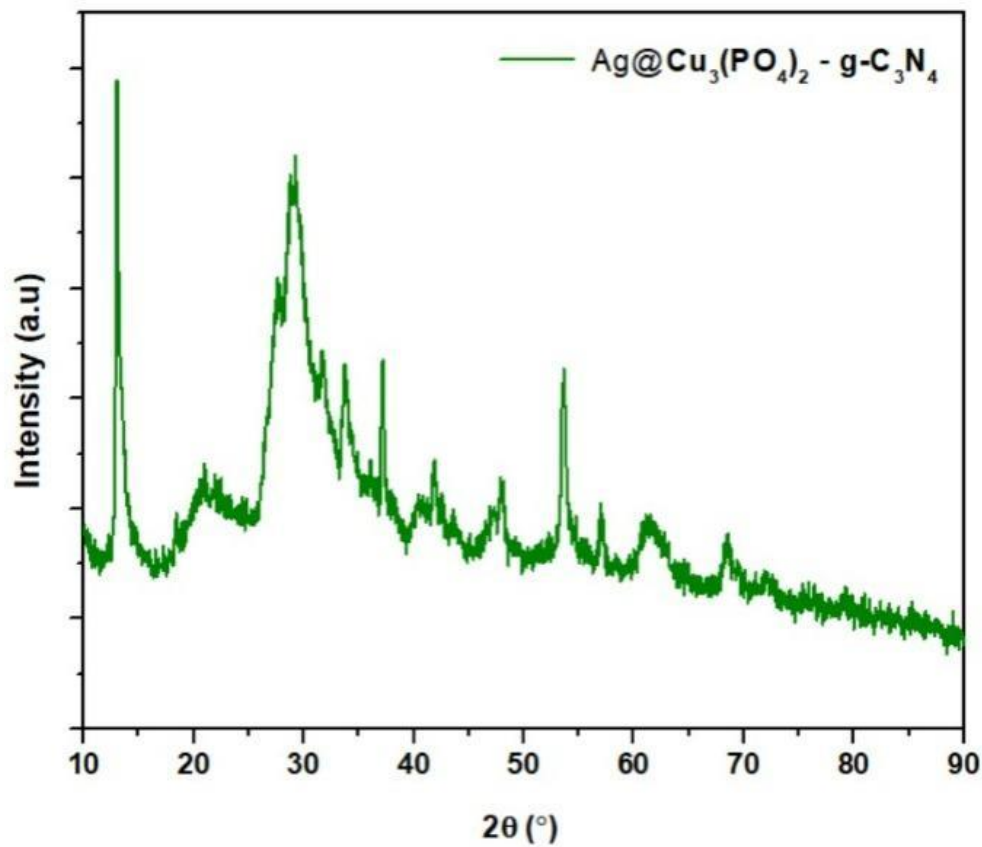


FIGURE 1: XRD (X-Ray Diffraction)

Figure 1 shows the XRD pattern which typically exhibits characteristic peaks that correspond to the arrangement of atoms within the crystal lattice of Ag@Cu<sub>3</sub>(PO<sub>4</sub>)<sub>2</sub>-gC<sub>3</sub>N<sub>4</sub>

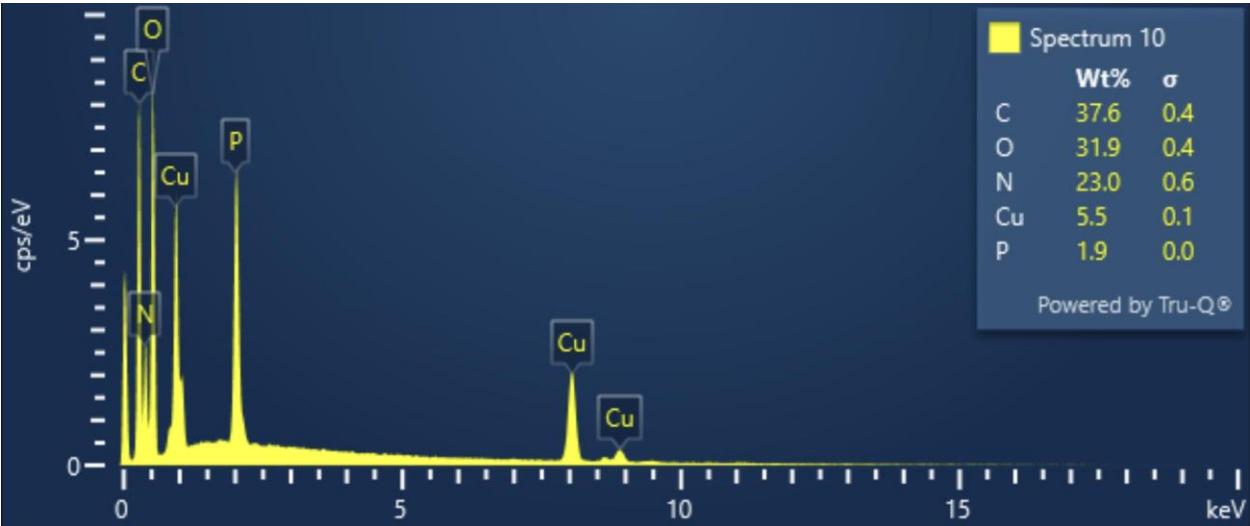


FIGURE 2 : EDS ANALYSIS

The graph shows the quantity of different components present in Ag@Cu<sub>3</sub>(PO<sub>4</sub>)<sub>2</sub>-gC<sub>3</sub>N<sub>4</sub>

**Spectrum 10**

Element	Line Type	Apparent Concentration	k Ratio	Wt%	Wt% Sigma	Standard Label	Factory Standard	Standard Calibration Date
C	K series	3.93	0.03926	37.62	0.41	C Vit	Yes	
N	K series	4.66	0.00830	23.03	0.57	BN	Yes	
O	K series	4.11	0.01382	31.94	0.36	SiO2	Yes	
P	K series	1.36	0.00759	1.93	0.03	GaP	Yes	
Cu	K series	2.30	0.02301	5.48	0.09	Cu	Yes	
Total:				100.00				

**FIGURE 3 : ELEMENTAL COMPOSITION**

The table shows the percentage by weight of various elements in Ag@Cu<sub>3</sub>(PO<sub>4</sub>)<sub>2</sub>-gC<sub>3</sub>N<sub>4</sub>

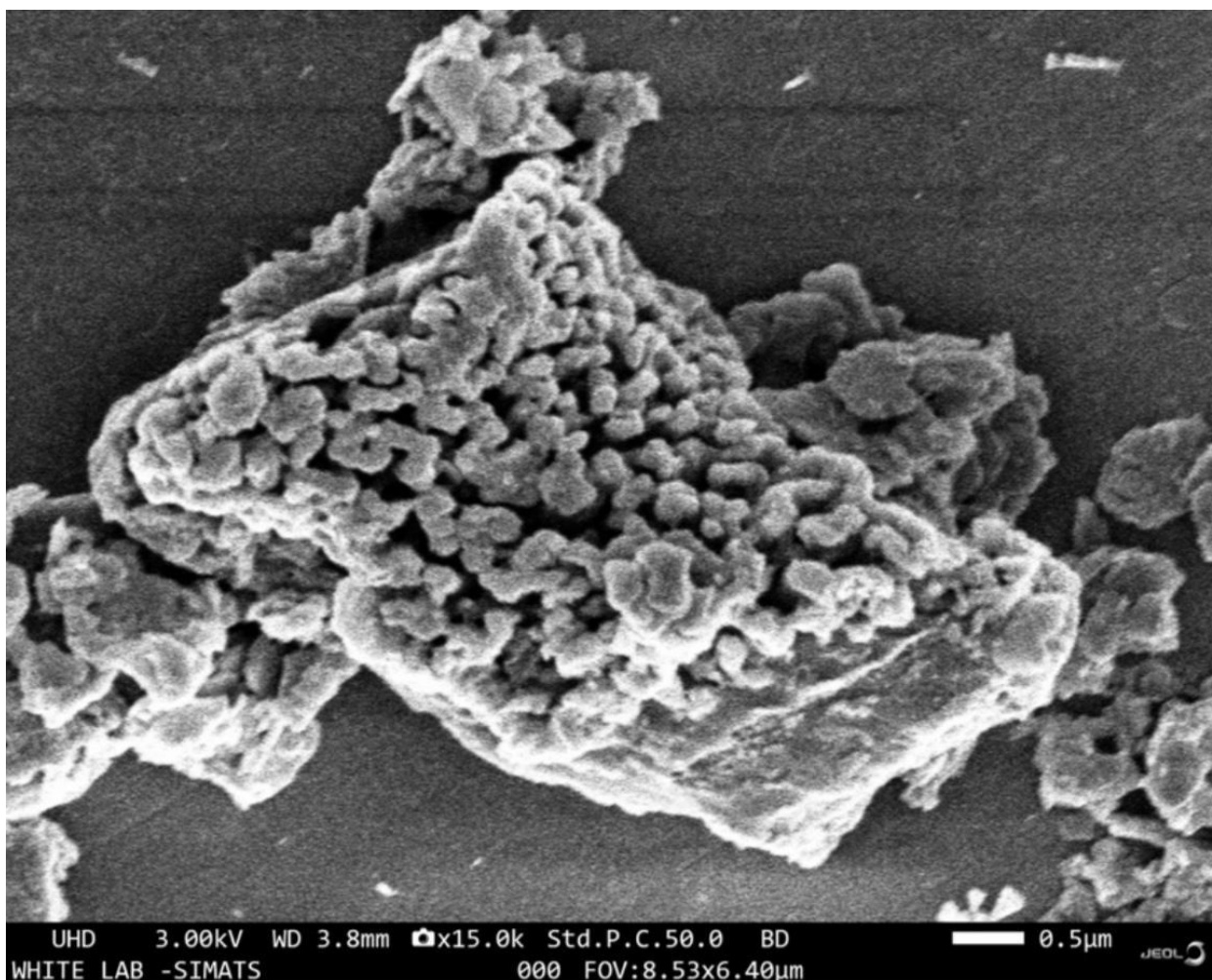
**FIGURE 4 : SEM IMAGE**

Figure 4 shows the SEM image of g-C<sub>3</sub>N<sub>4</sub>



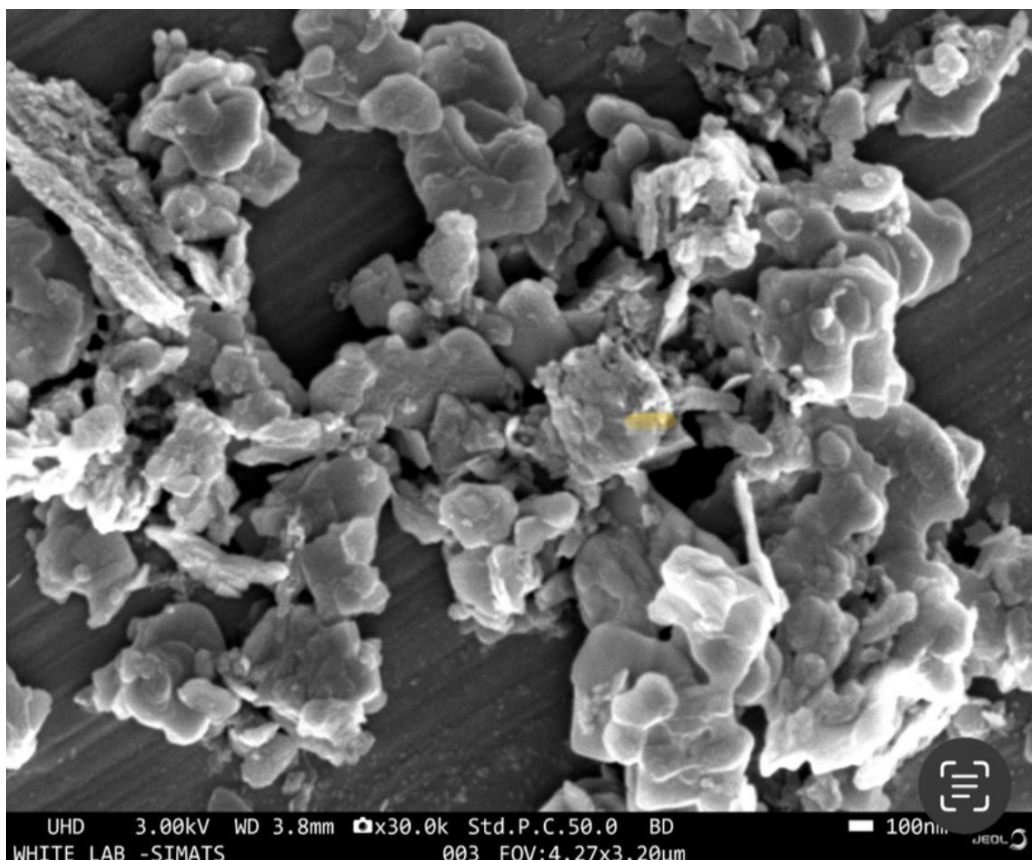


FIGURE 5 : SEM IMAGE

Figure shows the SEM image of Ag@Cu<sub>3</sub>(PO<sub>4</sub>)<sub>2</sub>-gC<sub>3</sub>N<sub>4</sub>

## Electron Image 10

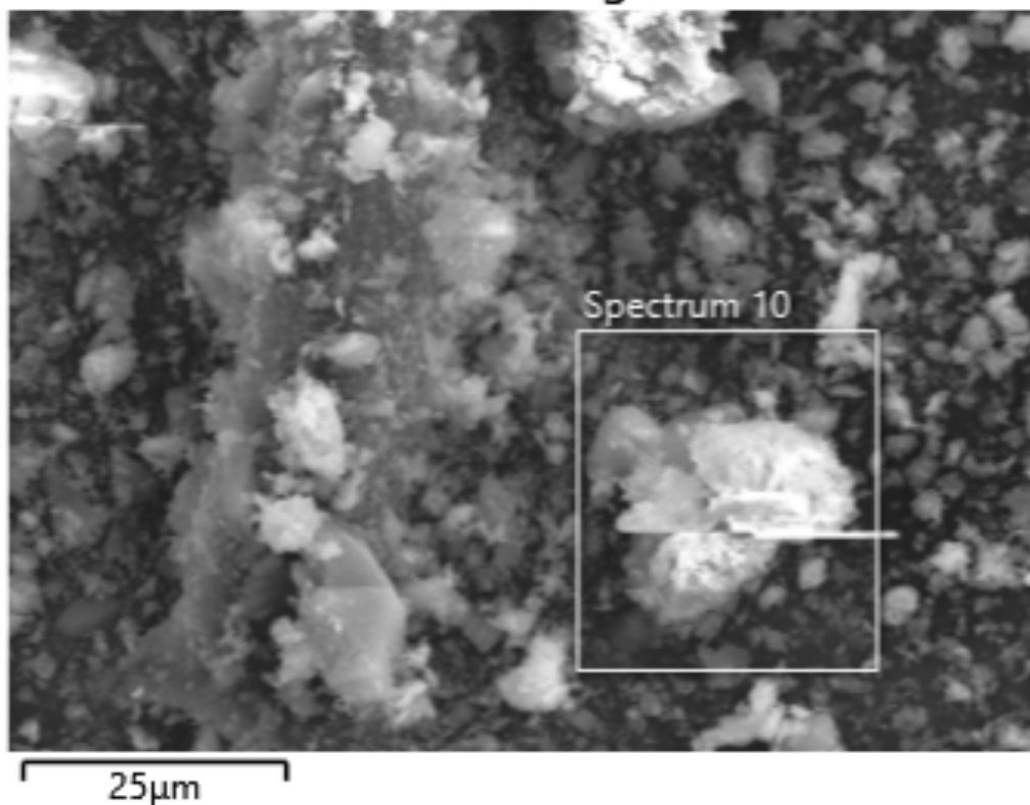


FIGURE 6 : ELECTRON MICROSCOPY IMAGE

The electron microscopy image shows surface morphology of Ag@Cu<sub>3</sub>(PO<sub>4</sub>)<sub>2</sub>-gC<sub>3</sub>N<sub>4</sub>

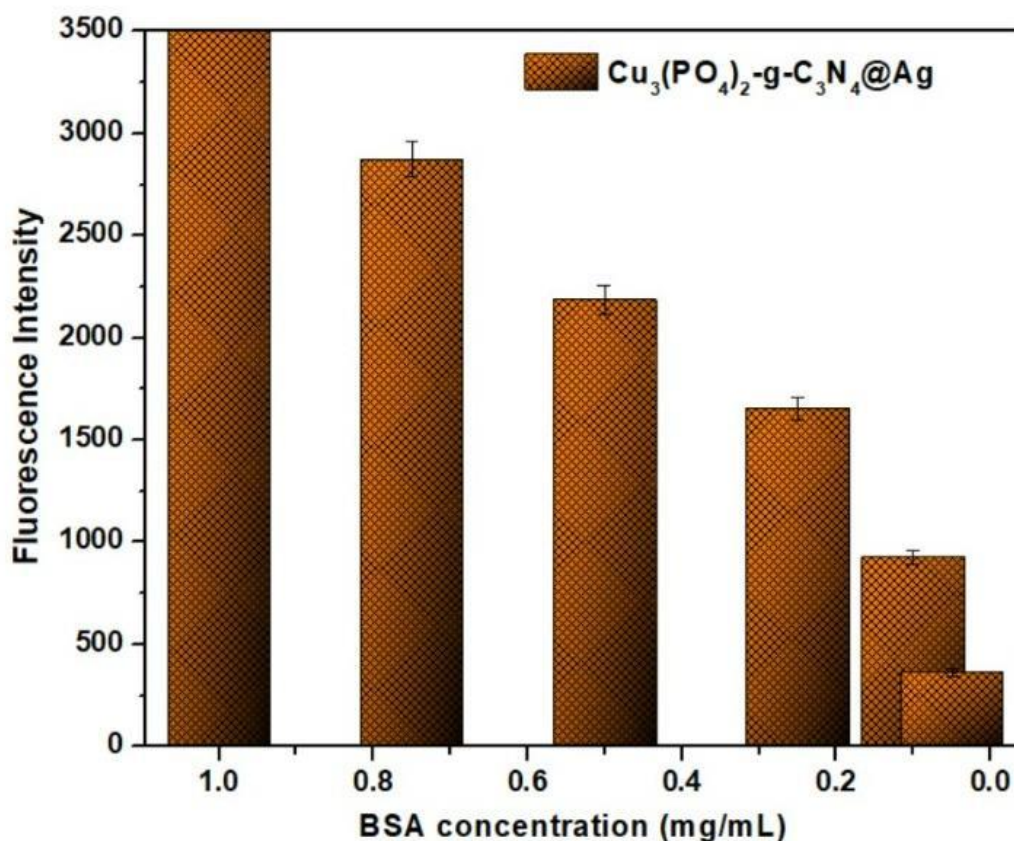


FIGURE 7 : BSA CONCENTRATION

Figure 7 shows the BSA concentration. In minimum BSA concentrations, the fabricated compound shows highest biosensing activity

## DISCUSSION

C<sub>3</sub>N<sub>4</sub> XRD pattern typically exhibits characteristic peaks that correspond to the arrangement of atoms within the crystal lattice. XRD pattern typically exhibits characteristic peaks that correspond to the arrangement of atoms within the crystal lattice. The specific positions and intensities of these peaks can provide valuable information about the crystal structure of C<sub>3</sub>N<sub>4</sub>. Cu<sub>3</sub>(PO<sub>4</sub>)<sub>2</sub> crystallizes in a monoclinic crystal system, and its XRD pattern usually exhibits A strong peak around  $2\theta = 16^\circ - 18^\circ$ , Several medium to strong peaks in the range of  $2\theta = 22^\circ - 32^\circ$ , Additional peaks with lower intensities at higher  $2\theta$  values, typically in the range of  $2\theta = 35^\circ - 60^\circ$ (9). These peaks correspond to the crystallographic planes within the material and can be used to determine the crystal structure. Silver (Ag) often displays a specific pattern of diffraction peaks according to its crystal structure in its X-ray diffraction (XRD) pattern. Face centered cubic structure, miller indices, and high intensity are the general descriptions of the silver XRD pattern(10).

EDS analysis shows that Ag@Cu<sub>3</sub>(PO<sub>4</sub>)<sub>2</sub>-gC<sub>3</sub>N<sub>4</sub> consists a composition( 37.62 % - carbon, 23.03% - nitrogen, 31.94% - oxygen, 1.93% - phosphorous and 5.48% - copper )of various components, which confirms the proper chemical formation of Ag@Cu<sub>3</sub>(PO<sub>4</sub>)<sub>2</sub>-gC<sub>3</sub>N<sub>4</sub>. The composite is likely to exhibit a layered or stratified structure(11). This layered arrangement can result from the combination of Ag nanoparticles, Cu<sub>3</sub>(PO<sub>4</sub>)<sub>2</sub>, and g-C<sub>3</sub>N<sub>4</sub> sheets. The surface may contain Ag nanoparticles that appear as small, discrete, and often spherical or irregularly shaped entities. These nanoparticles may be dispersed or clustered on the surface of the composite. Depending on the synthesis process, Cu<sub>3</sub>(PO<sub>4</sub>)<sub>2</sub> crystals may be present on the surface. They can exhibit distinct crystal facets and may appear

as larger, well-defined structures compared to the nanoparticles. The C<sub>3</sub>N<sub>4</sub> matrix is found to have many voids and silver particles according to SEM investigation, which expands the scope of the biosensing application(12).

Chitosan, ionic liquid, and graphene nanocomposites worked together synergistically to increase the sensor's sensitivity and electrochemical responsiveness. To characterize the sensor and look into its electrochemical response, various techniques including scanning electron microscopy (SEM), cyclic voltammetry (CV), electrochemical impedance spectrum (EIS), and differential pulse voltammetry (DPV) were applied(13). With a detection limit of 2 1011 g/L, the prepared MIPs/CS/IL-GR/GCE demonstrated a linear connection between the changes in current response and the logarithms of BSA concentrations in the range of 1.0 1010 to 1.0 104 g/L ( $R = 0.996$ ). Additionally, the manufactured sensor had high selectivity, outstanding stability, good reproducibility, and acceptable recovery, indicating possible use in the clinical field. The Fluorescence intensity shows the degree of quantification of Bovine serum albumin by the electrochemical biosensor(14). At a BSA concentration of (1.0, 0.8, 0.6, 0.4 and 0.2) the corresponding fluorescence intensity values are (3500nm, 2900nm, 2250nm, 1750nm and 800nm)(15).

## CONCLUSION

In our study, Ag compound is highly sensitive highly compatible high in strength and also highly selective. Because of using less amount Ag in results we didn't get EDX results positive. The composite material demonstrates positive results even at low concentrations of BSA, indicating its effectiveness for detecting and quantifying BSA in various samples. Nevertheless, the

research on Ag@Cu<sub>3</sub>(PO<sub>4</sub>)<sub>2</sub>-gC<sub>3</sub>N<sub>4</sub> biosensor for BSA detection provides a foundation for potential forensic applications in various areas of analysis and investigation. FUTURE SCOPE: Optimization of synthesis parameters, Characterization techniques, Electrochemical performance evaluation, Biosensor optimization.

### ACKNOWLEDGEMENTS

We would like to thank Saveetha Dental College and Hospitals, Saveetha Institute of Medical and Technical Sciences, Saveetha University for providing us support to conduct the study.

### CONFLICT OF INTEREST

The author declares that there were no conflicts of interests in the present study.

### SOURCE OF FUNDING

This project is funded by KSB architects & builders, Anna nagar, Chennai-600040.

### ETHICAL CLEARANCE

Since it is an in vitro study, ethical clearance number is not required.

### REFERENCES

1. Hammond JL, Formisano N, Estrela P, Carrara S, Tkac J. Electrochemical biosensors and nanobiosensors. *Essays Biochem*. 2016 Jun 30;60(1):69–80.
2. Clark LC Jr, Lyons C. Electrode systems for continuous monitoring in cardiovascular surgery. *Ann N Y Acad Sci*. 1962 Oct 31;102:29–45.
3. Jahanban-Esfahlan A, Ostadrahimi A, Jahanban-Esfahlan R, Roufegarinejad L, Tabibiazar M, Amarowicz R. Recent developments in the detection of bovine serum albumin. *Int J Biol Macromol*. 2019 Oct 1;138:602–17.
4. Zhang M, Naik RR, Dai L. Carbon Nanomaterials for Biomedical Applications. Springer; 2015. 576 p.
5. Nag A, Mukhopadhyay SC, Kosel J. Printed Flexible Sensors: Fabrication, Characterization and Implementation. Springer; 2019. 198 p.
6. Naresh V, Lee N. A Review on Biosensors and Recent Development of Nanostructured Materials-Enabled Biosensors. *Sensors [Internet]*. 2021 Feb 5;21(4). Available from: <http://dx.doi.org/10.3390/s21041109>
7. Nunes D, Pimentel A, Santos L, Barquinha P, Pereira L, Fortunato E, et al. Metal Oxide Nanostructures: Synthesis, Properties and Applications. Elsevier; 2018. 328 p.
8. Ozkan SA, Bakirhan NK, Mollaraosouli F. The Detection of Biomarkers: Past, Present, and the Future Prospects. Academic Press; 2021. 614 p.
9. Mollamohammadi F, Faridnouri H, Zare EN. Electrochemical Biosensing of L-DOPA Using Tyrosinase Immobilized on Carboxymethyl Starch--Polyaniline@MWCNTs Nanocomposite. *Biosensors [Internet]*. 2023 May 21;13(5). Available from: <http://dx.doi.org/10.3390/bios13050562>
10. Dourandish Z, Sheikshoae I, Maghsoudi S. Molybdenum Disulfide/Nickel-Metal Organic Framework Hybrid Nanosheets Based Disposable Electrochemical Sensor for Determination of 4-Aminophenol in Presence of Acetaminophen. *Biosensors [Internet]*. 2023 May 7;13(5). Available from: <http://dx.doi.org/10.3390/bios13050524>
11. Matusiewicz H, Bulska E. Inorganic Trace Analytics: Trace Element Analysis and Speciation. Walter de Gruyter GmbH & Co KG; 2017. 459 p.
12. Pye K. Geological and Soil Evidence: Forensic Applications. CRC Press; 2007. 356 p.
13. Zinggeler M, Schär S, Kurth F. Printed Antifouling Electrodes for Biosensing Applications. *ACS Appl Mater Interfaces*. 2022 Dec 28;14(51):56578–84.
14. Dong H, Zheng M, Chen M, Song D, Huang R, Zhang A, et al. Exploiting the size exclusion effect of protein adsorption layers for electrochemical detection of microRNA: A new mechanism for design of E-DNA sensor. *Biosens Bioelectron*. 2023 Jan 15;220:114911.
15. Ensafi AA. Electrochemical Biosensors. Elsevier; 2019. 388 p.
16. Sneka S, Preetha Santhakumar. Antibacterial Activity of Selenium Nanoparticles extracted from Capparis decidua against Escherichia coli and Lactobacillus Species. *Research Journal of Pharmacy and Technology*. 2021; 14(8):4452-4. doi: 10.52711/0974-360X.2021.00773
17. Vishaka S, Sridevi G, Selvaraj J. An in vitro analysis on the antioxidant and anti-diabetic properties of Kaempferia galanga rhizome using different solvent systems. *J Adv Pharm Technol Res*. 2022 Dec;13(Suppl 2):S505-S509. doi: 10.4103/japtr.japtr\_189\_22.
18. Sankar S. In silico design of a multi-epitope Chimera from Aedes aegypti salivary proteins OBP 22 and OBP 10: A promising candidate vaccine. *J Vector Borne Dis*. 2022 Oct-Dec;59(4):327-336. doi: 10.4103/0972-9062.353271.
19. Devi SK, Paramasivam A, Girija ASS, Priyadharsini JV. Decoding The Genetic Alterations In Cytochrome P450 Family 3 Genes And Its Association With HNSCC. *Gulf J Oncolog*. 2021 Sep;1(37):36-41.